Magnetic and dielectric properties of hexagonal $InMnO_3$

Alexei A. Belik,[1,*] Stanislav Kamba,[2] Maxim Savinov,[2] Dmitry Nuzhnyy,[2] Makoto Tachibana,[3] Eiji Takayama-Muromachi,[1,3] and V. Goian[2]

[1]*International Center for Materials Nanoarchitectonics (MANA), National Institute for Materials Science (NIMS), , 1-1 Namiki, Tsukuba, Ibaraki 305-0044, Japan*

[2]*Institute of Physics, ASCR, v.v.i. Na Slovance 2, 18221 Prague 8, Czech Republic*

[3]*Superconducting Materials Center, National Institute for Materials Science (NIMS), 1-1 Namiki, Tsukuba, Ibaraki 305-0044, Japan*

(Received 17 October 2008; published 11 February 2009)

High quality ceramics of hexagonal $InMnO_3$ were prepared using a high-pressure and high-temperature technique (at 6 GPa and 1373 K). Magnetic properties of $InMnO_3$ were investigated using dc and ac magnetizations and specific heat. High-temperature behavior was studied with differential scanning calorimetry, differential thermal analysis, time-domain terahertz (THz) transmission, and infrared reflectivity spectroscopies. Antiferromagnetic long-range magnetic order takes place below $T_N=118$ K with very weak anomalies on magnetic susceptibilities and a strong anomaly on specific heat. No change in specific heat was found at a magnetic field of 7 T. Very weak ferromagnetic properties were detected below T_N. High-temperature (above 250 K) low-frequency permittivity is strongly enhanced by the Maxwell-Wagner polarization but intrinsic permittivity measured in a THz range shows only small linear increase with temperature up to 900 K. Ferroelectric hysteresis loop measurements (below 250 K) revealed no spontaneous polarization; therefore, $InMnO_3$ is nonferroelectric. Absence of a structural phase transition is also supported by infrared reflectivity studies (taken up to 850 K). However, low-frequency permittivity exhibits an anomaly near T_N giving evidence about a magnetoelectric coupling.

DOI: 10.1103/PhysRevB.79.054411 PACS number(s): 75.47.Lx, 75.50.Ee, 75.40.Cx, 77.22.Ch

I. INTRODUCTION

Recently, there has been a revival of interest in multiferroic materials.[1,2] In magnetoelectric multiferroic materials, magnetism and (anti)ferroelectricity coexist.[1] Among various multiferroic materials, hexagonal (space-group $P6_3cm$) manganites $RMnO_3$ (R=Sc, In, Y, and Ho-Lu) are particularly interesting because of the specific origin of ferroelectricity,[3] coupling between different order parameters,[2] and frustrated magnetism.[4] There are a lot of experimental and theoretical works on hexagonal $RMnO_3$ with R=Sc, Y, and Ho-Lu.[2–24] The ferroelectric (FE) phase transition in these compounds takes place at high temperatures above 1100–1200 K.[5–9] Note that the ferroelectric phase-transition temperatures are still a matter of debate in the literature (for the same composition, quite different values are given).[5–10] Because Mn^{3+} ions form a triangular lattice, there is strong magnetic frustration. Mn^{3+} ions in $RMnO_3$ order antiferromagnetically ($T_N=130$ K for $ScMnO_3$ and $T_N=70-75$ K for $YMnO_3$) in the 120° structure with the same magnetic and chemical unit cells (propagation vector $\boldsymbol{k}=[0,0,0]$).[6,11–13]

To the best of our knowledge, there are only four papers about hexagonal $InMnO_3$.[25–28] The very limited number of works on $InMnO_3$ is probably related to difficulties in preparation of $InMnO_3$.[26] The lattice parameters of $InMnO_3$ have anomalies compared with other compounds in the series: the a lattice parameter (=5.8758 Å) is smaller than expected, and the c lattice parameter (=11.4715 Å) is larger than expected.[26] Very weak anomalies were observed on the magnetic susceptibilities near 15, 40, and 120 K.[26,27] Broad magnetic reflections on neutron powder-diffraction patterns appeared below 120 K with the propagation vector $\boldsymbol{k}=[0,0,1/2]$.[26] The propagation vector in $InMnO_3$ is different compared with other $RMnO_3$ compounds. The magnetic reflections were assigned to two-dimensional short-range order, and the absence of long-range order in $InMnO_3$ was postulated.[26] In Ref. 27, it is reported that $T_N=15$ K.

Another work has reported that long-range antiferromagnetic order with weak ferromagnetism takes place at $T_N=50$ K in $InMnO_3$, and a FE transition occurs at T_{CE} near 500 K.[28] Unfortunately, no information about the sample preparation, sample purity, and quality was reported in Ref. 28; moreover, no discussion of the reported magnetic properties compared with those of Ref. 26 was given. In the first works on $ScMnO_3$, a weak ferromagnetic signal was observed below 40–50 K with hysteresis on the M vs H curves.[11,12] Later, it was shown that ferromagneticlike anomalies near 40–50 K are related to the ferrimagnetic impurity of Mn_3O_4, and pure samples showed anomalies only near T_N.[14] For example, reheating at 1170 K in flowing O_2 produced impurity-free $ScMnO_3$ samples.[14] In good $RMnO_3$ (R=Sc, Y, and Ho-Lu) powder samples, very weak or no anomalies were detected at T_N on magnetic-susceptibility curves while specific-heat measurements clearly showed the onset of magnetic ordering.[12–14]

Magnetic and dielectric properties of hexagonal $InMnO_3$ are still not clarified and controversial compared with those of $RMnO_3$ (R=Sc, Y, and Ho-Lu). In this work, we report the preparation of high quality samples of hexagonal $InMnO_3$ using a high-pressure technique, and its magnetic properties studied with dc and ac magnetizations and specific heat. The FE phase transition occurs according to Ref. 28 near 500 K, and because low-frequency dielectric data can be strongly influenced by conductivity at such high temperature, we perform high-frequency experiments in a terahertz (THz) range up to 900 K to clarify the nature of the ferroelectric phase transition without influence of conductivity. We will show

that, based on dielectric measurements, $InMnO_3$ is not ferroelectric but it shows a dielectric anomaly near $T_N=118$ K giving evidence about a magnetoelectric coupling.

II. EXPERIMENTAL

A stoichiometric mixture of In_2O_3 (99.9%) and Mn_2O_3 was placed in Au capsules, and treated at 6 GPa in a belt-type high-pressure apparatus at 1373 K for 30 min (heating rate of 110 K/min). After heat treatment, the samples were quenched to room temperature (RT), and the pressure was slowly released. The resultant samples were black dense pellets. Single-phase Mn_2O_3 was prepared from a commercial MnO_2 (99.99%) by heating in air at 923 K for 24 h. X-ray powder-diffraction (XRD) data of $InMnO_3$ collected at RT on a RIGAKU Ultima III diffractometer using Cu K_α radiation (2θ range of 5–100°, a step width of 0.02°, and a counting time of 10 s/step) showed that the samples contained a very small amount (1 wt. %) of cubic In_2O_3 as an impurity. The lattice parameters were refined by the Rietveld method with RIETAN-2000 [$a=5.8818(1)$ Å and $c=11.4810(5)$ Å].[29]

$InGaO_3$ with space-group $P6_3/mmc$ [the refined lattice parameters of our sample are $a=3.3103(1)$ Å and $c=12.0469(5)$ Å] (Ref. 30) has a structure corresponding to a paraelectric phase of $RMnO_3$ (R=Sc, Y, In, and Ho-Lu) and, therefore, we used $InGaO_3$ for estimation of the lattice contribution to the specific heat of $InMnO_3$. Single-phase $InGaO_3$ was prepared from In_2O_3 and Ga_2O_3 (99.9%) powders at 6 GPa and 1373 K for 1 h.

dc magnetic susceptibilities, $\chi=\mathbf{M}/\mathbf{H}$, of $InMnO_3$ were measured on a superconducting quantum interference device (SQUID) magnetometer [Quantum Design, Magnetic Property Measurement System (MPMS)] between 2 and 350 K in applied fields of 0.01, 1, and 7 T under both zero-field-cooled (ZFC) and field-cooled (FC) (on cooling) conditions, and between 300 and 700 K in an applied field of 5 T on heating. Isothermal magnetization measurements were performed between −7 and 7 T at 5 K. Frequency dependent ac susceptibility measurements at zero static magnetic field were performed with a MPMS instrument from 200 to 2 K at frequencies (f) of 0.5, 2, 7, 25, 110, and 300 Hz, and an applied oscillating magnetic field (H_{ac}) of 5 Oe. No frequency dependence was found. Specific heat, C_p, of $InMnO_3$ at 0 and 7 T was measured between 2 and 300 K on cooling by a pulse relaxation method using a commercial calorimeter [Quantum Design, Physical Property Measurement System (PPMS)].

For the time-domain THz transmission experiments, we used a Ti:sapphire femtosecond laser oscillator. Linearly polarized THz probing pulses were generated by an interdigitated photoconducting switch from GaAs and detected using the electro-optic sampling with a 1-mm-thick [110] ZnTe crystal. The complex dielectric spectra were taken in the range of 8–55 cm^{-1} (240 GHz–1.65 THz) at temperatures from 300 to 900 K. Low-frequency (100 Hz–1 MHz) dielectric measurements were performed between 10 and 300 K using an impedance analyzer HP 4192A. In the same temperature range, ferroelectric hysteresis loops at frequencies of 1–50 Hz were investigated.

Near-normal infrared (IR) reflectivity spectra were obtained using a Fourier transform IR spectrometer Bruker IFS 113 in the frequency range of 50–650 cm^{-1} (1.5–19.5 THz), i.e., in the range of polar-phonon frequencies. The IR measurements were performed up to 850 K using a commercial high-temperature sample cell SPECAC P/N 5850. The same cell was used also for high-temperature THz experiment.

Differential scanning calorimetry (DSC) curves of $InMnO_3$ were recorded on a SII Exstar 6000 (DSC 6220) system at a heating/cooling rate of 10 K/min from 290 to 873 K (two runs) in semiclosed aluminum capsules. The first heating DSC curve of $InMnO_3$ showed a very broad anomaly between 625 and 750 K. However, no anomalies were found on the cooling curves and the second heating curve. Therefore, the origin of the anomalies in $InMnO_3$ on the first heating curve is likely to be annealing effects observed in many samples prepared at high pressure.[31] The XRD data collected after the DSC experiment showed no change in the phase composition. The thermal stability of $InMnO_3$ in air was also examined on a SII Exstar 6000 (TG-DTA 6200; TG is thermogravimetry) system between 290 and 1340 K at a heating/cooling rate of 10 K/min using Pt holders. No anomalies were found on the differential thermal analysis (DTA) curves. The XRD data collected after the TG/DTA experiment showed the presence of cubic In_2O_3 (~8.5 wt %) and Mn_3O_4 (~5.0 wt %) phases in addition to hexagonal $InMnO_3$.

III. RESULTS AND DISCUSSION

Figure 1 shows dc magnetic susceptibilities of $InMnO_3$ between 2 and 700 K. Small increase in the χ values with difference between the ZFC and FC curves was observed below $T_N=118$ K. Very weak and broad anomalies were detected near 55 K at 0.01 T. However at 1 and 7 T, there were no anomalies near 55 K. A broad maximum was observed below 118 K on the ZFC curves at 0.01 and 1 T; however, no such feature was detected at the 7 T ZFC curve. At 7 T, there was only a kink at 118 K.

We note that some of our lower quality $InMnO_3$ samples [containing (In,Mn)OOH and rhombohedral In_2O_3 as detectable (by XRD) impurities] showed anomalies on magnetic susceptibilities near 15 and 40 K, that is, at the same temperatures as anomalies found in Refs. 26–28. Therefore, anomalies near 15 and 40 K are most probably extrinsic, and our high-pressure sintering technique can produce high quality $InMnO_3$ samples.

The inverse magnetic susceptibilities of $InMnO_3$ in the temperature range of 300–700 K were fit by the Curie-Weiss equation,

$$\chi(T) = \chi_0 + \mu_{\text{eff}}^2 N[3k_B(T-\theta)]^{-1}, \quad (1)$$

where $\mu_{\text{eff}}[=4.88(7)\mu_B]$ is effective magnetic moment, N is Avogadro's number, k_B is Boltzmann's constant, $\theta[=-768(19)$ K] is the Weiss constant, and $\chi_0[=1.5(4)\times10^{-4}$ $cm^3/mol]$ is the temperature-independent term. The effective magnetic moment is very close to the expected value of $4.90\mu_B$ for Mn^{3+}. The ratio $|\theta/T_N|=6.5$ indicates the presence of frustration. Note that, because of the large $|\theta|$

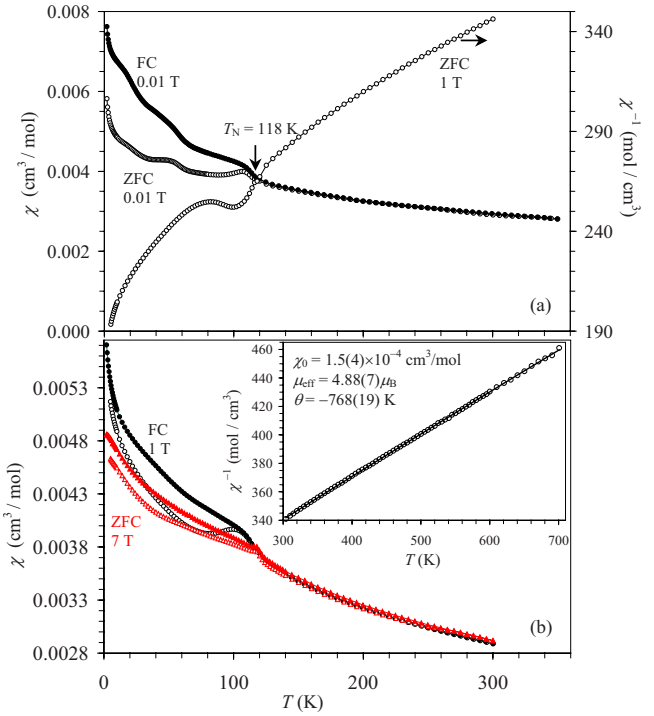

FIG. 1. (Color online) (a) ZFC and FC dc magnetic-susceptibility (χ=**M**/**H**) curves of $InMnO_3$ measured at 10^{-2} T (the left-hand scale) and the inverse ZFC magnetic-susceptibility curve measured at 1 T (the right-hand scale). (b) ZFC (white symbols) and FC (full symbols) dc magnetic-susceptibility curves of $InMnO_3$ measured at 1 T (circles) and 7 T (triangles). The inset gives the χ^{-1} vs T curve (symbols) measured at 5 T from 300 to 700 K. The line shows the fit to Eq. (1) with parameters given on the figure.

values in hexagonal manganites, the reliable parameters can be obtained by fitting in a high-temperature region,[14,26] and inverse magnetic susceptibilities below about 300 K show noticeable deviation from the linear Curie-Weiss behavior [Fig. 1(a)].

Close examination of the ZFC curves at 0.01 and 1 T showed that there were two anomalies: at 118 and 110 K, respectively. This feature is more clearly seen on the ac susceptibility curves of $InMnO_3$ (Fig. 2). The χ' vs T curve showed broad maxima centered at 110 and 118 K. The χ'' vs T curve demonstrated a maximum only below 110 K indicating the appearance of a weak ferromagnetic moment. Anomalies were also observed near 55 K on both χ' vs T and χ'' vs T curves in agreement with the dc magnetization measurements at 0.01 T. The anomalies near 55 K are probably originated from a very small amount of magnetic impurities[11] undetectable by XRD.

Figure 3 depicts the isothermal magnetization curves at 5 K. The M vs H curves are basically linear. A very small hysteresis is observed with the coercive field (H_c) of about 0.015 T and the remnant magnetization (M_r) of about 1.3 $\times 10^{-4}\mu_B$ per formula unit (during the ZFC M vs H measurements from 0 to 1 T, from 1 to −1 T, and from −1 to 1 T). The magnetic moment reaches only $0.06\mu_B$ per formula unit at 7 T.

Figure 4 shows the specific heat of $InMnO_3$ at 0 T plotted as C_p/T vs T. There was no detectable difference at 7 T

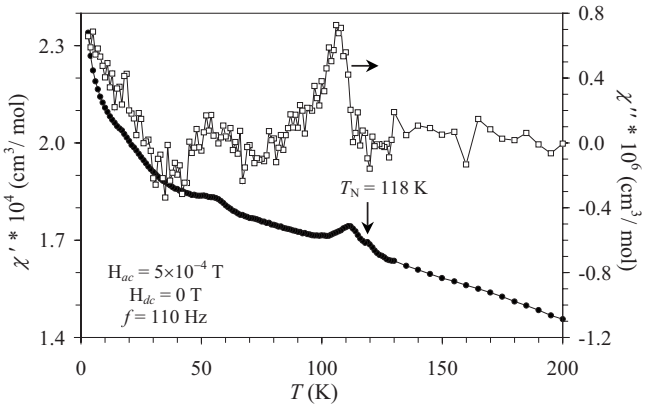

FIG. 2. Real χ' and imaginary χ'' parts of the ac susceptibility as a function of temperature (2–200 K) for $InMnO_3$. Measurements were performed on cooling at zero static field using the ac field with the amplitude $H_{ac}=5\times10^{-4}$ T and frequency $f=110$ Hz.

similar to the specific heat of $YMnO_3$, $LuMnO_3$, and $ScMnO_3$.[14] This fact shows that magnetic field (at least up to 7 T) has a very small effect on antiferromagnetic ordering.[19] The characteristic peak (λ-type anomaly on the C_p vs T) was observed at 118 K indicating the onset of long-range ordering. The lattice contribution (C_L) in $InMnO_3$ was estimated in two ways. First, we used the raw specific-heat data of $InGaO_3$ containing no magnetic ions [$C_L(1)$]. The magnetic specific heat [$C_m(1)$] of $InMnO_3$ is obtained by subtracting the total specific heat of $InGaO_3$ from that of $InMnO_3$ [$C_m = C_p - C_L$]. The magnetic entropy was obtained using the equation

$$S_m = \int (C_m/T)dT. \tag{2}$$

$S_m(1)$ estimated in the first way is 14.2 J K^{-1} mol^{-1} (referred to the value at 300 K) that is slightly larger than the spin-only value of $R\ln(2S+1)=R\ln 5=13.38$ J K^{-1} mol^{-1} expected for the $S=2$ systems (S is spin). As seen from Fig. 4, this discrepancy is obviously from the poor lattice estimation above 200 K.

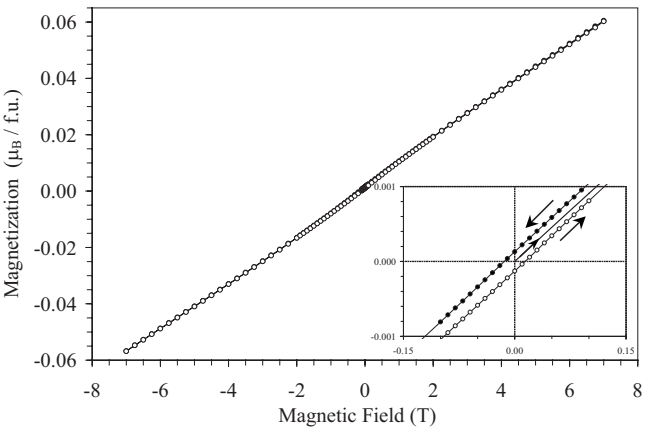

FIG. 3. Isothermal magnetization curves of $InMnO_3$ at 5 K. The inset shows the curves near the origin.

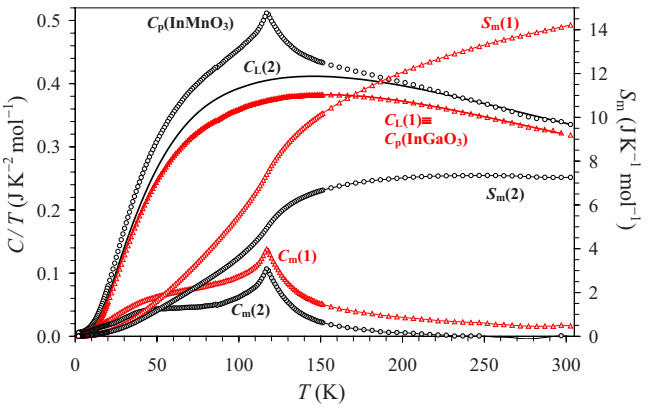

FIG. 4. (Color online) C_p/T vs T, C_m/T vs T, and S_m vs T curves of $InMnO_3$ at 0 T between 2 and 300 K (C_m is magnetic specific heat and S_m is magnetic entropy). The C_p/T vs T curve of $InGaO_3$ (triangle symbols) gives the first lattice estimation [$C_L(1)$, see the text]; the line shows the fit with Eq. (3). $C_L(2)$ presents the second lattice estimation (see the text). $C_m(1)/T$ and $S_m(1)$ were obtained using $C_L(1)$, and $C_m(2)/T$ and $S_m(2)$ using $C_L(2)$. See the text for detailed explanation.

The specific-heat data plotted as C_p/T^3 vs T showed broad maxima at 24 K in $InGaO_3$ and 20 K in $InMnO_3$ (Fig. 5). The similar broad peak was observed in the specific heat of $LuMnO_3$.[15] Bumps were also found near 50 K on the C_m/T vs T curves of $YMnO_3$, $LuMnO_3$, and $ScMnO_3$.[14] The appearance of broad peaks and bumps was first assigned to the magnetic contribution from Mn^{3+} at low temperature due to strong frustration. However, it was shown later that broad maxima on the C_p/T^3 vs T curves are not related to Mn^{3+} ions (or anomalous magnetic contribution) but come from the specific lattice contribution that is usually neglected.[16] In most cases, the Debye approximation is used to estimate C_L. This approximation works well for systems dominated by acoustic phonons. However, very often additional contributions are present from optical modes (Einstein contribution to the excitation spectrum). $InGaO_3$ has no magnetic ions and it exhibits a broad maximum on the C_p/T^3 vs T curve. This fact clearly shows the presence of the Einstein contribution in C_L of $InMnO_3$.

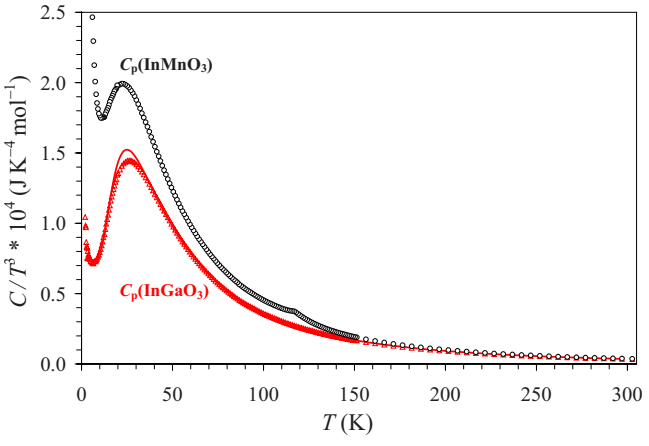

FIG. 5. (Color online) C_p/T^3 vs T curves of $InMnO_3$ (circle symbols) and $InGaO_3$ (triangle symbols) at 0 T between 2 and 300 K. The line shows the fit with Eq. (3) for $InGaO_3$.

Therefore, we fitted the C_p vs T data of $InGaO_3$ between 2 and 300 K using the equation

$$C_L = D(\theta_{D1}, n_{D1}) + D(\theta_{D2}, n_{D2}) + E(\theta_E, n_E), \qquad (3)$$

where D is the Debye function with the Debye temperature of θ_D and the oscillator strength of n_D, and E is the Einstein function with the Einstein temperature of θ_E and the oscillator strength of n_E. It was shown that two Debye functions are necessary to give good fitting in the whole temperature range. A good fit (Figs. 4 and 5) was obtained with reasonable parameters (θ_E=123 K and n_E=0.8/f.u.,[16] θ_{D1}=882 K and n_{D1}=9.7/f.u., and θ_{D2}=355 K and n_{D2}=4.5/f.u.).[14] Then we fit the C_p vs T data of $InMnO_3$ between 200 and 300 K with Eq. (3) with fixed θ_E, n_E, n_{D1}, and n_{D2} or fixed θ_E, n_E, θ_{D1}, n_{D1}, and θ_{D2}. Both fittings gave similar estimation of $C_L(2)$ (the second way of estimation). $S_m(2)$ estimated in the second way is 7.3 J K^{-1} mol^{-1} that is noticeably smaller than the spin-only value. This is probably related to the magnetic frustration. The way of estimation of C_L had no principal effect on the form of the C_m/T vs T curves of $InMnO_3$, that is, no bumps were found on the C_m/T vs T curves of $InMnO_3$ below T_N compared with the data for $ScMnO_3$.[14] However, we believe that $C_L(2)$ was estimated in a more reasonable way, giving the more reliable $S_m(2)$ value.

To the best of our knowledge, the only paper with the synthesis and properties of $InGaO_3$ reported that its resistivity (0.015 Ω cm at RT) is temperature independent between 4 and 300 K.[30] This result is quite surprising. Therefore, we think it is necessary to comment on it. The specific-heat measurements of $InGaO_3$ showed a negligible linear contribution to the specific heat. Our resistivity measurements on ceramic $InGaO_3$ samples showed a semiconductor-type behavior. Therefore, the reported peculiar electrical behavior of $InGaO_3$ in Ref. 30 is probably of extrinsic origin.

Magnetic susceptibilities and specific heat of $InMnO_3$ are similar with those of other hexagonal manganites; that is, there is a small anomaly near T_N on magnetic susceptibilities and a strong anomaly on specific heat. The specific-heat data confirmed the onset of long-range magnetic order. Therefore, the appearance of magnetic reflections on neutron powder-diffraction patterns below 120 K should be considered as confirmation of three-dimensional magnetic order rather than two-dimensional short-range order.[26] The broadening of magnetic reflections observed in Ref. 26 can probably be explained by difficulties in preparation of samples with good crystallinity at ambient pressure [according to our results, $InMnO_3$ starts to decompose around 1300 K in air (see below); but synthesis of $RMnO_3$ requires annealing at 1270–1670 K]. The magnetic structure of $InMnO_3$ with the propagation vector $\boldsymbol{k}$=[0,0,1/2] should be different from those of other hexagonal manganites with the propagation vector $\boldsymbol{k}$=[0,0,0] and requires special investigations.

The magnetic transition temperatures T_N decrease in $RMnO_3$ with increasing radius of R^{3+} ions [T_N=130 K with $r_{VI}(Sc^{3+})$=0.745 Å,[32] T_N=90 K with $r_{VI}(Lu^{3+})$=0.861 Å, and T_N=71 K with $r_{VI}(Y^{3+})$=0.900 Å].[14] $InMnO_3$ with T_N=118 K and $r_{VI}(In^{3+})$=0.800 Å is in agreement with this tendency.

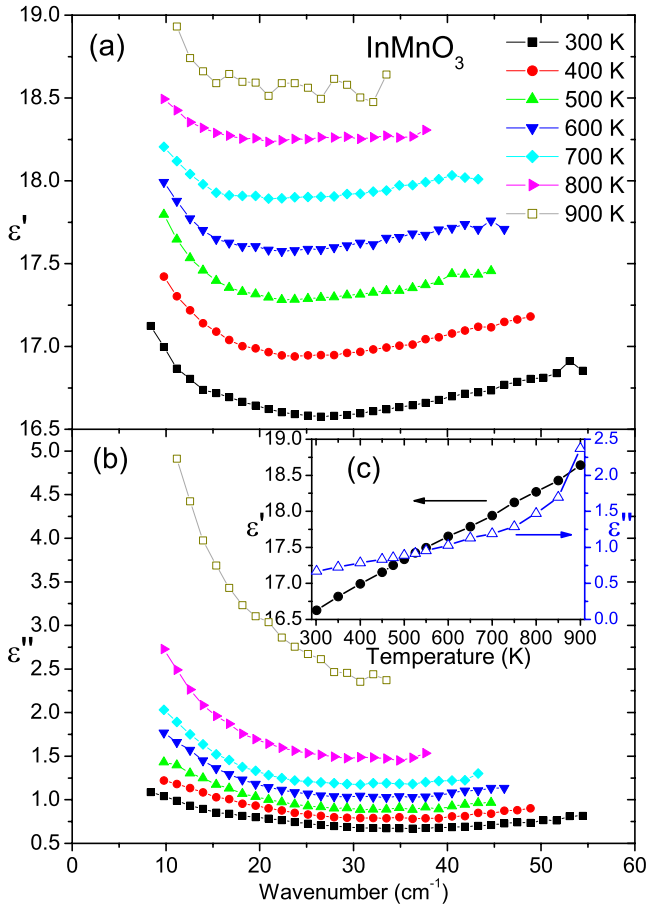

FIG. 6. (Color online) Frequency dependence of (a) real and (b) imaginary parts of complex permittivity in a THz range at different temperatures. The inset (c) shows temperature dependence of ε' and ε'' measured at 1 THz on heating.

No anomalies were found on the DSC curves between 300 and 870 K (except for the first heating curve); moreover, the phase composition did not change. No anomalies were also found on the complex dielectric permittivity measured at 1 THz between 300 and 900 K (inset of Fig. 6). The permittivity increases gradually from about 16.6 at 300 K to 18.6 at 900 K while a peak in THz $\varepsilon'(T)$ should be seen in the case of a displacive ferroelectric phase transition. Such permittivity values of $InMnO_3$ are in agreement with those of other hexagonal manganites $RMnO_3$ (R=Sc, Y, and Lu) (ε =15–22 at 150 K).[14,15] The small increase in permittivity with temperature is caused by slight shift of several phonon frequencies to lower values (i.e., phonon softening) observed in IR reflectivity spectra (see Fig. 7). Mainly the phonon near 155 cm^{-1} exhibits 10 cm^{-1} shift down. It follows from sum rule for oscillator strengths f_j of polar phonons,

$$f = \sum f_j = \sum \Delta\varepsilon_j(T)\omega_j^2(T) = \text{const}. \quad (4)$$

Here $\Delta\varepsilon_j$ and ω_j denote dielectric strength (or contribution to static permittivity) and eigenfrequency of the jth polar phonon, respectively. In the case when the phonons are not coupled, which is a frequent case, each f_j is temperature independent [i.e., $\Delta\varepsilon_j(T)\omega_j^2(T)$=const]. It means that each

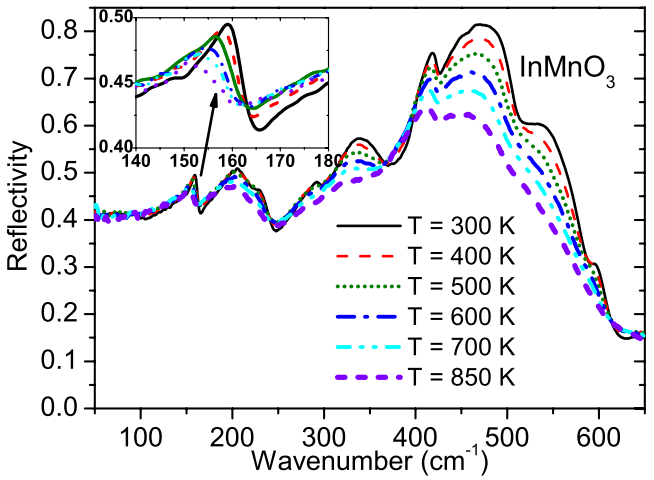

FIG. 7. (Color online) Infrared reflectivity spectra of $InMnO_3$ taken at various temperatures. Shift of lowest frequency phonon with temperature seen in inset is responsible for the small increase in THz permittivity with rising temperature (see inset of Fig. 6).

reduction in phonon frequency ω_j results in increase in dielectric strength $\Delta\varepsilon_j$.

THz spectra in Fig. 6 clearly show not only phonon contribution (see the increase in ε' with rising frequency above 25 cm^{-1}) but also another excitation below 20 cm^{-1} which can be caused by microwave dielectric relaxation or conductivity. The latter possibility is more probable because conductivity and the related Maxwell-Wagner polarization strongly influence low-frequency dielectric data in Ref. 28 (see discussion below).

We have to stress that changes in a crystal structure, which are necessary at a ferroelectric phase transition, are always accompanied by changes in selection rules for activity of polar phonons in IR spectra.[33] However, no phonons disappear from the IR spectra at high temperatures (see Fig. 7), giving the evidence that the structure does not change at least up to 850 K.

The reported observation of huge increase in low-frequency permittivity (ε' up to 10^3–10^4) (Ref. 28) and its very strong frequency dependence (reported below 50 kHz) in $InMnO_3$ are typical for extrinsic contributions, e.g., defect induced conductivity inducing the so-called Maxwell-Wagner polarization,[34] which is responsible for relaxorlike behavior observed in Ref. 28. Therefore, our results do not confirm the ferroelectric phase transition at 500 K seen in Ref. 28.

For suppression of the Maxwell-Wagner polarization influence on ε', we performed low-frequency dielectric measurements below 300 K (see Fig. 8). One can see that the intrinsic permittivity can be measured below 250 K even at 10 kHz and that the permittivity (like in a THz range) is much lower than that of Ref. 28 at RT (~70). Nevertheless, low value of ε' does not exclude ferroelectricity. Therefore we performed polarization hysteresis loop measurements at various temperatures (see Fig. 9). No ferroelectric but just loss dielectric behavior was observed. Note two shapes of hysteresis loops taken at 250 K. An ellipsoid with two sharp heads (similar to the reported curves in Ref. 28) was ob-

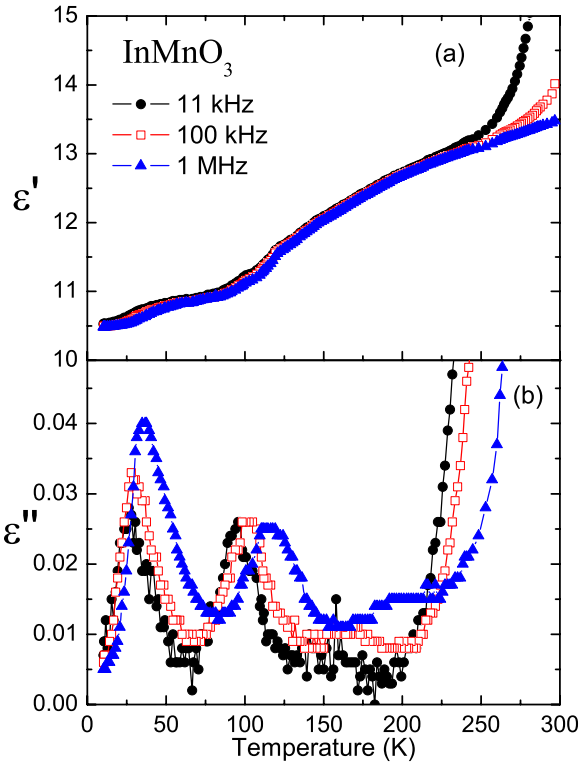

FIG. 8. (Color online) Temperature dependence of (a) real and (b) imaginary parts of complex permittivity below room temperature.

tained in the case of the triangular-shaped increase and decrease in the applied voltage. However, in the case of the sinusoidal change in the voltage, only a smooth ellipsoid, corresponding to loss dielectric, was observed. The ellipsoid narrows on cooling but it cannot be compensated down to 50 K. Nevertheless, the hysteresis loops are not ferroelectric, and, therefore, $InMnO_3$ behaves only as paraelectric in the studied temperature and electric-field ranges despite the fact that $InMnO_3$ belongs to the family of ferroelectric materials from the structural point of view.

The permittivity of $InMnO_3$ shows a curvature at T_N [Fig. 8(a)]; this curvature is very similar to the anomalies observed in $LuMnO_3$ and $YMnO_3$ at T_N.[14,15] The anomaly near T_N gives evidence about the magnetoelectric coupling in $InMnO_3$. Two dielectric relaxations are clearly seen in dielectric loss ε'' spectra below T_N and below 50 K [Fig. 8(b)]. The second relaxation probably comes from the magnetic

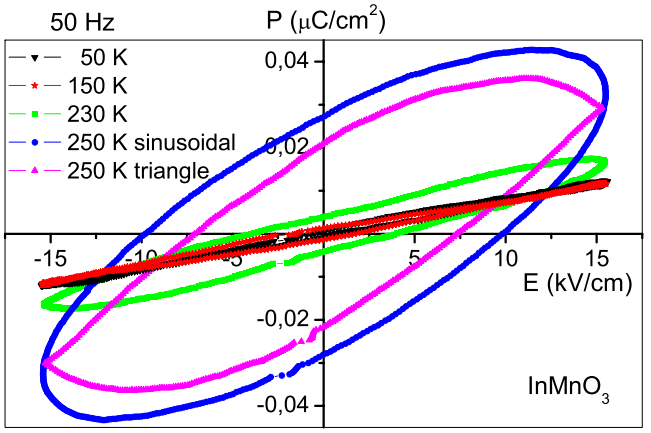

FIG. 9. (Color online) Polarization hysteresis loops taken at various temperatures. Different shape of two loops taken at 250 K is caused by different kinds of applied electric voltage.

impurity detected by magnetic-susceptibility measurements in our ceramic $InMnO_3$ samples.

No DTA anomalies were found in $InMnO_3$ up to 1340 K; however after the DTA experiment, the sample contained hexagonal $InMnO_3$, and impurities of In_2O_3 and Mn_3O_4. This fact shows that $InMnO_3$ gradually decomposes at high temperatures, confirming the difficulties in the ambient-pressure synthesis of $InMnO_3$. The formation of Mn_3O_4 can explain the magnetic anomalies observed near 40–50 K in samples prepared at ambient pressure.[26–28]

In conclusion, magnetic properties of hexagonal $InMnO_3$ were studied by dc and ac magnetizations and specific-heat measurements. We found that long-range antiferromagnetic order takes place below T_N=118 K. Dielectric and differential scanning calorimetry studies disprove the ferroelectric/structural phase transition earlier reported near 500 K, and moreover they give evidence that the sample is not multiferroic. $InMnO_3$ is just a paraelectric antiferromagnet but the dielectric anomaly observed near T_N gives evidence about magnetoelectric coupling so the sample is magnetoelectric.

ACKNOWLEDGMENTS

This work was supported by World Premier International Research Center (WPI) Initiative on Materials Nanoarchitectonics (MEXT, Japan) and by the NIMS Individual-Type Competitive Research Grant. Support from the Czech Science Foundation (Projects No. 202/06/0403 and No. AVOZ10100520) is acknowledged.

*Author to whom correspondence should be addressed. International Center for Materials Nanoarchitectonics (MANA), National Institute for Materials Science, Namiki 1-1, Tsukuba, Ibaraki, 305-0044, Japan. Alexei.BELIK@nims.go.jp

[1] R. Ramesh and N. A. Spaldin, Nature Mater. **6**, 21 (2007).
[2] T. Lottermoser, T. Lonkai, U. Amann, D. Hohlwein, J. Ihringer, and M. Fiebig, Nature (London) **430**, 541 (2004).
[3] B. B. Van Aken, T. T. M. Palstra, A. Filippetti, and N. A. Spaldin, Nature Mater. **3**, 164 (2004).
[4] M. Fiebig, D. Frohlich, K. Kohn, S. Leute, T. Lottermoser, V. V. Pavlov, and R. V. Pisarev, Phys. Rev. Lett. **84**, 5620 (2000).
[5] S. C. Abrahams, Acta Crystallogr., Sect. B: Struct. Sci. **57**, 485 (2001).
[6] T. Katsufuji, M. Masaki, A. Machida, M. Moritomo, K. Kato, E. Nishibori, M. Takata, M. Sakata, K. Ohoyama, K. Kitazawa, and H. Takagi, Phys. Rev. B **66**, 134434 (2002).

[7] Th. Lonkai, D. G. Tomuta, U. Amann, J. Ihringer, R. W. A. Hendrikx, D. M. Tobbens, and J. A. Mydosh, Phys. Rev. B **69**, 134108 (2004).
[8] G. Nenert, M. Pollet, S. Marinel, G. R. Blake, A. Meetsma, and T. T. M. Palstra, J. Phys.: Condens. Matter **19**, 466212 (2007).
[9] I.-K. Jeong, N. Hur, and Th. Proffen, J. Appl. Crystallogr. **40**, 730 (2007).
[10] N. Fujimura, T. Ishida, T. Yoshimura, and T. Ito, Appl. Phys. Lett. **69**, 1011 (1996).
[11] M. Bieringer and J. E. Greedan, J. Solid State Chem. **143**, 132 (1999).
[12] A. Munoz, J. A. Alonso, M. J. Martinez-Lope, M. T. Casais, J. L. Martinez, and M. T. Fernandez-Diaz, Phys. Rev. B **62**, 9498 (2000).
[13] A. Munoz, J. A. Alonso, M. J. Martinez-Lope, M. T. Casais, J. L. Martinez, and M. T. Fernandez-Diaz, Chem. Mater. **13**, 1497 (2001).
[14] D. G. Tomuta, S. Ramakrishnan, G. J. Nieuwenhuys, and J. A. Mydosh, J. Phys.: Condens. Matter **13**, 4543 (2001).
[15] T. Katsufuji, S. Mori, M. Masaki, Y. Moritomo, N. Yamamoto, and H. Takagi, Phys. Rev. B **64**, 104419 (2001).
[16] M. Tachibana, J. Yamazaki, H. Kawaji, and T. Atake, Phys. Rev. B **72**, 064434 (2005).
[17] H. D. Zhou, J. A. Janik, B. W. Vogt, Y. J. Jo, L. Balicas, M. J. Case, C. R. Wiebe, J. C. Denyszyn, J. B. Goodenough, and J. G. Cheng, Phys. Rev. B **74**, 094426 (2006).
[18] H. D. Zhou, J. Lu, R. Vasic, B. W. Vogt, J. A. Janik, J. S. Brooks, and C. R. Wiebe, Phys. Rev. B **75**, 132406 (2007).
[19] F. Yen, C. dela Cruz, B. Lorenz, E. Galstyan, Y. Y. Sun, M. Gospodinov, and C. W. Chu, J. Mater. Res. **22**, 2163 (2007).
[20] M. Fiebig, D. Frohlich, T. Lottermoser, and R. V. Pisarev, Phys. Rev. B **65**, 224421 (2002).
[21] M. Fiebig, C. Degenhardt, and R. V. Pisarev, J. Appl. Phys. **91**, 8867 (2002).
[22] Y. V. Golikov, V. F. Balakirev, S. G. Titova, O. M. Fedorova, and A. V. Antonov, Inorg. Mater. **41**, 524 (2005).
[23] H. W. Xu, J. Iwasaki, T. Shimizu, H. Satoh, and N. Kamegashira, J. Alloys Compd. **221**, 274 (1995).
[24] T. J. Sato, S. H. Lee, T. Katsufuji, M. Masaki, S. Park, J. R. D. Copley, and H. Takagi, Phys. Rev. B **68**, 014432 (2003).
[25] D. M. Giaquinta and H. C. zur Loye, J. Am. Chem. Soc. **114**, 10952 (1992).
[26] J. E. Greedan, M. Bieringer, J. F. Britten, D. M. Giaquinta, and H. C. zur Loye, J. Solid State Chem. **116**, 118 (1995).
[27] G. V. Vajenine, R. Hoffmann, and H. C. zur Loye, Chem. Phys. **204**, 469 (1996).
[28] C. R. Serrao, S. B. Krupanidhi, J. Bhattacharjee, U. V. Waghmare, A. K. Kundu, and C. N. R. Rao, J. Appl. Phys. **100**, 076104 (2006).
[29] F. Izumi and T. Ikeda, Mater. Sci. Forum **321-324**, 198 (2000).
[30] R. D. Shannon and C. T. Prewitt, J. Inorg. Nucl. Chem. **30**, 1389 (1968).
[31] A. A. Belik, T. Wuernisha, T. Kamiyama, K. Mori, M. Maie, T. Nagai, Y. Matsui, and E. Takayama-Muromachi, Chem. Mater. **18**, 133 (2006).
[32] R. D. Shannon, Acta Crystallogr., Sect. A: Cryst. Phys., Diffr., Theor. Gen. Crystallogr. **32**, 751 (1976).
[33] E. Buixaderas, S. Kamba, and J. Petzelt, Ferroelectrics **308**, 131 (2004).
[34] J. F. Scott, J. Mater. Res. **22**, 2053 (2007).